

## Unsteady MHD Casson Fluid Flow with Ramped Wall Temperature and Ramped Surface Concentration over Exponential Flow Embedded in a Porous Medium

Hari R. Kataria<sup>1</sup>, Rakesh R Darji<sup>2</sup>

<sup>1</sup>Department Of Mathematics, Faculty of Science,  
The M. S. University of Baroda, Vadodara, India  
<sup>1</sup>hrkrmaths@yahoo.com

<sup>2</sup>Applied Science & Humanities Department,  
Sardar Vallabhbhai Patel Institute of Technology, Vasad, India  
<sup>2</sup>darjirakesh12@gmail.com

**Corresponding author** <sup>2</sup>(+91-9879750932)

### Abstract

The present paper is concerned with the study of flow, heat and mass transfer characteristics in the unsteady magneto hydrodynamics Casson fluid flow past over an exponential vertical plate. The governing partial differential equations are solved analytically using Laplace transform. The features of the fluid flow, heat and mass transfer characteristics are analyzed by plotting graphs and the physical aspects are discussed in detail. The results obtained show the impact of Prandtl number  $Pr$ , Grashof number  $Gr$ , Mass Grashof number  $Gm$ , Schmidt number  $Sc$ , Casson parameter  $\gamma$ , magnetic parameter  $M$ , permeability of porous medium  $K$  and time  $t$  on velocity, heat and mass transfer.

**Keywords:** Magneto hydrodynamics; Casson fluid; Ramped temperature; Ramped Surface.

**AMS Subject Classification:** 76W05

### Introduction:

The problems of magneto hydrodynamic free convective flow in a porous medium have drawn considerable attentions of several researchers in various scientific and technological applications such as pumps, flow meters, generators, accelerators, plasma jet engines, and magnetic control of molten iron flow in steel industry and industrial processes in metallurgy and material processing, in chemical industry, industrial power engineering and nuclear engineering. Special mention can be made, for

instance, to the experiments on liquid metal flows in MHD channels performed by J. Hartmann and F. Lazarus (1937) et al. [1], the discovery of Alfvén waves finalized the establishment of MHD as an individual science by H. Alfvén (1942) [2]. Raptis have determined *MHD free convection flow past an accelerated vertical plate*. Kataria and Mittal [3-4] have studied an exact solution for unsteady MHD free convection flow on nano fluid. M. Sheikholeslami *et al.* [5] studied the numerical simulation of nano fluid forced convection heat transfer improvement in existence of magnetic field. In modern engineering, many flow characteristics are not explainable with the Newtonian fluid model. Hence non-Newtonian fluid theory has become useful, but a single equation cannot cover all physical properties of such fluids. The governing equations are highly nonlinear. Also, the industrial applications of non-Newtonian fluid flow are increasing day by day. Among the many industrial non-Newtonian fluids some fluids behave like elastic solids, and for those fluids, a yield shear stress exists in the constitutive equations. Casson fluid is one of such fluids. So if the shear stress magnitude is greater than yield shear stress, then flow occurs. Kataria and Patel [6] discussed the effect of magnetic field on unsteady natural convective flow of a micropolar fluid between two vertical walls. Kataria and Patel [7-8] have studied the effect of heat and mass transfer in second grade fluid. Hayat et al. [9] solved exact solutions of second grade aligned MHD fluid with prescribed vorticity. Hayat et al. [10] also discussed three-dimensional flow of second grade nanofluid by a convectively heated exponentially stretching surface. Bataineh et al [11] have developed Bernstein method for the MHD flow and heat transfer of a second grade fluid in a channel with porous wall. Kataria and Patel [12-13] also discussed effects on MHD Casson fluid flow past an oscillating vertical plate embedded in porous medium. Malik et al. [14] have solved variable viscosity and MHD flow in Casson fluid with Cattaneo–Christov heat flux model: Using Keller box method. Nadeem et al. [15-16] have determined solution of MHD Casson fluid flow past over a porous medium. Mukhopadhyaya et al. [17-18] studied casson fluid flow over an unsteady stretching surface. Khalid [19] discussed unsteady MHD free convection flow of Casson fluid past over an oscillating vertical plate. Rosseland [20] studied Astrophysik und atom-theoretische Grundlagen.

The purpose of this paper is to analyze the important role of concentration in MHD flow of a casson fluidflow past over an exponential vertical plate with ramped wall temperature and ramped wall surface. We find the analytic solution using Laplace transform technique.

#### **Nomenclature:**

- $u$  - Velocity of the fluid in the  $x$  direction,
- $T$  - Temperature,
- $C$  - Concentration,
- $g$  - Acceleration due to gravity,
- $k_1$  - Permeability,
- $c_p$  - Specific heat of the fluid at constant pressure,

- D - Mass diffusivity,
- Sc - Schmidt Number,
- Pr - Prandtl Number,
- Gm - Grashof Number of Mass transfer,
- Gr - Grashof Number
- t - Time

**Greek Alphabets:**

- $\gamma$  - Casson parameter
- $\beta$  - Volumetric coefficient of thermal expansion
- $\sigma$  - Electric conductivity of the fluid
- $\rho$  - Density,
- $\emptyset$  - Porosity of the fluid
- k - Thermal conductivity,
- $\mu\beta$  - Plastic dynamic viscosity,
- $\nu$  - Kinematic viscosity,

**Mathematical Formulation of the Problem:**

We consider casson fluid past on exponential vertical plate with concentration in porous medium. The flow being confined to  $y > 0$ , where  $y$  is the coordinate measured in the normal direction to the plate and  $x - axis$  is taken along the wall in the upward direction. A uniformly distributed transverse magnetic field of strength  $B_0$  is applied in the  $y - axis$  direction. Induced magnetic field produced by the fluid motion is negligible in comparison with the applied one as the magnetic Reynolds number is small enough to neglect the effects of applied magnetic field. Initially, at time  $t = 0$ , both the fluid and the plate are uniform temperature  $T_\infty$  and the concentration near the plate is assumed to be  $C_\infty$  respectively. At time  $t > 0$ , the plate begins to oscillate in its own plane according to  $e^{a't}$ ,  $T_\infty + (T_w + T_\infty)t/t_0$  when  $t \leq t_0$  and  $T_w$  when  $t > t_0$  respectively and Concentration near the plate is raised linearly to  $C_w$  which is thereafter maintained constant  $T_w$  &  $C_w$ . We assume that, rigid plate, incompressible flow, one dimensional flow, non-Newtonian fluid, free convection, oscillating vertical plate and viscous dissipation term in the energy equation is neglected.

The constitutive equation for the Casson fluid can be written as

$$\tau_{ij} = \begin{cases} 2 \left( \mu B + \frac{Py}{\sqrt{2\pi}} \right) e_{ij} & \pi > \pi_c \\ 2 \left( \mu B + \frac{Py}{\sqrt{2\pi_c}} \right) e_{ij} & \pi < \pi_c \end{cases}$$

Where  $\pi = e_{ij}e_{ij}$  and  $e_{ij}$  is the  $(i, j)^{\text{th}}$  component of the deformation rate,  $\pi$  is the product of the component of deformation rate with itself,  $\pi_c$  is a critical value of this product based on the non-Newtonian model,  $\mu B$  is plastic dynamic viscosity of the non-Newtonian fluid and  $P_y$  is yield stress of fluid. Under these conditions we get the following partial differential equation with initial and boundary conditions are given below.

$$\frac{\partial u}{\partial t} = \mu B \left( 1 + \frac{1}{\gamma} \right) \frac{\partial^2 u}{\partial y^2} - \sigma B_0^2 u - \frac{\mu \varphi}{k_1} u + \rho g \beta (T - T_\infty) + g \beta_c (C - C_\infty) C \quad (1)$$

$$\rho c_p \frac{\partial T}{\partial t} = k \frac{\partial^2 T}{\partial y^2} \quad (2)$$

$$\frac{\partial C}{\partial t} = D \frac{\partial^2 C}{\partial y^2} \quad (3)$$

With initial and boundary condition

$$u = 0, \quad T = T_\infty, \quad C = C_\infty; \text{ as } y \geq 0 \text{ and } t < 0$$

$$u = e^{a't}, \quad T = \begin{cases} T_\infty + (T_w - T_\infty) t/t_0 & \text{if } 0 < t < t_0 \\ T_w & \text{if } t \geq t_0 \end{cases}, \quad C = C_\infty + (C_w - C_\infty);$$

$$\text{as } t \geq 0 \text{ and } y = 0$$

$$u \rightarrow 0, T \rightarrow T_\infty, \quad C \rightarrow C_\infty; \text{ as } y \rightarrow \infty \text{ and } t \geq 0 \quad (4)$$

Introducing the following dimensionless quantities:

$$y' = \frac{U}{v t_0} y, \quad t' = \frac{U^2 t}{v t_0}, \quad u' = \frac{\sqrt{t_0}}{U} u, \quad \theta = \frac{T - T_\infty}{T_w - T_\infty}, \quad C = \frac{C - C_\infty}{C_w - C_\infty}, \quad w' = \frac{w v}{U^2}, \quad \tau' = \frac{\tau}{\rho u^2}$$

In the equations (1-4) dropping out the " ' " notation (for simplicity) we get

$$\frac{\partial u}{\partial t} = \left( 1 + \frac{1}{\gamma} \right) \frac{\partial^2 u}{\partial y^2} - \left( M^2 + \frac{1}{k} \right) u + Gr\theta + GmC \quad (5)$$

$$p_r \frac{\partial \theta}{\partial t} = \frac{\partial^2 \theta}{\partial y^2} \quad (6)$$

$$\frac{\partial C}{\partial t} = \frac{1}{Sc} \frac{\partial^2 C}{\partial y^2} \quad (7)$$

With initial and boundary condition

$$u = \theta = C = 0, \quad y \geq 0, t = 0$$

$$u = e^{a't}, \quad \theta = \begin{cases} t, & 0 < t \leq 1 \\ 1 & t > 1 \end{cases} = tH(t) - (t-1)H(t-1),$$

$$C = \begin{cases} t, & 0 < t \leq 1 \\ 1 & t > 1 \end{cases} = tH(t) - (t-1)H(t-1), \quad y = 0, \quad t > 0$$

$$u \rightarrow 0, \theta \rightarrow 0, C \rightarrow 0 \quad \text{as } y \rightarrow \infty, t > 0 \quad (8)$$

Where

$H(\cdot)$  is Heaviside unit step function.

$$Pr = \frac{\mu c_p}{k}, M^2 = \frac{\sigma B_0^2}{\rho U^2} t_0, \quad \frac{1}{k} = \frac{v \phi^2}{k_1 U^2}, Gr = \frac{v g \beta (T_w - T_\infty)}{U^3}, \quad \gamma = \frac{\mu_B \sqrt{2\pi c}}{P_\gamma},$$

$$Sc = \frac{\nu}{D}, Gm = g \beta_c \nu (C_w - C_\infty)$$

**Solution:**

Taking Laplace transform of equation (5-7) with initial and boundary condition equations (8) we get

$$\bar{\theta} = \frac{1-e^{-s}}{s^2} e^{-y\sqrt{pr}s} \quad (9)$$

$$\bar{C} = \frac{e^{-y\sqrt{sc}s}}{s^2} \quad (10)$$

$$\bar{u} = \frac{1}{s-a} e^{-y\sqrt{\frac{s+b}{a}}} + \frac{1}{s^2} \frac{a_6(1-e^{-s})}{(s-a_5)} \left( e^{-y\sqrt{\frac{s+b}{a}}} - e^{-y\sqrt{pr}s} \right) + \frac{1}{s^2} \frac{a_9(1-e^{-s})}{(s-a_8)} \left( e^{-y\sqrt{\frac{s+b}{a}}} - e^{-y\sqrt{sc}s} \right) \quad (11)$$

Where

$$a = 1 + \frac{1}{\gamma}, \quad b = M^2 + \frac{1}{k}, \quad \frac{Gr}{a} = a_1, \quad \frac{Gm}{a} = a_2, \quad pr - \frac{1}{a} = a_3, \quad \frac{b}{a} = a_4, \quad \frac{a_4}{a_3} = a_5, \quad \frac{a_1}{a_3} = a_6,$$

$$sc - \frac{1}{a} = a_7, \quad \frac{a_4}{a_7} = a_8, \quad \frac{a_2}{a_7} = a_9$$

$$\bar{u} = G_1(y, s) + H_1(y, s)(1 - e^{-s}) \quad (12)$$

$$\text{Where } G_1(y, s) = \frac{1}{s-a} e^{-y\sqrt{\frac{s+b}{a}}} \quad (13)$$

$$H_1(y, s) = G_2(y, s) + G_3(y, s) + G_4(y, s) \quad (14)$$

$$G_2(y, s) = a_{10}F_1(y, s) + a_{12}F_2(y, s) - a_{14}F_3(y, s) - a_{15}F_4(y, s) \quad (15)$$

$$G_3(y, s) = a_{10}F_5(y, s) - a_{10}F_6(y, s) + a_{11}F_7(y, s) \quad (16)$$

$$G_4(y, s) = a_{12}F_8(y, s) - a_{12}F_9(y, s) + a_{13}F_{10}(y, s) \quad (17)$$

$$\text{Where } a_{10} = \frac{a_6}{a_5^2}, \quad a_{11} = \frac{a_6}{a_5}, \quad a_{12} = \frac{a_9}{a_8^2}, \quad a_{13} = \frac{a_9}{a_8}, \quad a_{10} + a_{12} = a_{14}, \quad a_{11} + a_{13} = a_{15}$$

$$F_1(y, s) = \frac{e^{-y\sqrt{\frac{s+b}{a}}}}{s-a_5} \quad (18)$$

$$F_2(y, s) = \frac{e^{-y\sqrt{\frac{s+b}{a}}}}{s-a_8} \quad (19)$$

$$F_3(y, s) = \frac{e^{-y\sqrt{\frac{s+b}{a}}}}{s} \quad (20)$$

$$F_4(y, s) = \frac{e^{-y\sqrt{\frac{s+b}{a}}}}{s^2} \quad (21)$$

$$F_5(y, s) = \frac{e^{-y\sqrt{pr}s}}{s} \quad (22)$$

$$F_6(y, s) = \frac{e^{-y\sqrt{p_r s}}}{s - a_5} \quad (23)$$

$$F_7(y, s) = \frac{e^{-y\sqrt{p_r s}}}{s^2} \quad (24)$$

$$F_8(y, s) = \frac{e^{-y\sqrt{s_c s}}}{s} \quad (25)$$

$$F_9(y, s) = \frac{e^{-y\sqrt{s_c s}}}{s - a_8} \quad (26)$$

$$F_{10}(y, s) = \frac{e^{-y\sqrt{s_c s}}}{s^2} \quad (27)$$

Inverse Laplace transforms of equations (13) and (18-27) are

$$g_1(y, t) = \frac{e^{a't}}{2} \left[ e^{-y\sqrt{\frac{b+a'}{a}}} \operatorname{erfc} \left( \frac{y}{2\sqrt{at}} - \sqrt{(b+a')t} \right) + e^{y\sqrt{\frac{b+a'}{a}}} \operatorname{erfc} \left( \frac{y}{2\sqrt{at}} + \sqrt{(b+a')t} \right) \right] \quad (28)$$

$$f_1(y, t) = \frac{e^{a_5 t}}{2} \left[ e^{-y\sqrt{\frac{b+a_5}{a}}} \operatorname{erfc} \left( \frac{y}{2\sqrt{at}} - \sqrt{(b+a_5)t} \right) + e^{y\sqrt{\frac{b+a_5}{a}}} \operatorname{erfc} \left( \frac{y}{2\sqrt{at}} + \sqrt{(b+a_5)t} \right) \right] \quad (29)$$

$$f_2(y, t) = \frac{e^{a_8 t}}{2} \left[ e^{-y\sqrt{\frac{b+a_8}{a}}} \operatorname{erfc} \left( \frac{y}{2\sqrt{at}} - \sqrt{(b+a_8)t} \right) + e^{y\sqrt{\frac{b+a_8}{a}}} \operatorname{erfc} \left( \frac{y}{2\sqrt{at}} + \sqrt{(b+a_8)t} \right) \right] \quad (30)$$

$$f_3(y, t) = \frac{1}{2} \left[ e^{-y\sqrt{\frac{b}{a}}} \operatorname{erfc} \left( \frac{y}{2\sqrt{at}} - \sqrt{bt} \right) + e^{y\sqrt{\frac{b}{a}}} \operatorname{erfc} \left( \frac{y}{2\sqrt{at}} + \sqrt{bt} \right) \right] \quad (31)$$

$$f_4(y, t) = \frac{1}{2} \left[ \left( t - \frac{y}{2\sqrt{ab}} \right) e^{-y\sqrt{\frac{b}{a}}} \operatorname{erfc} \left( \frac{y}{2\sqrt{at}} - \sqrt{bt} \right) + \left( t + \frac{y}{2\sqrt{ab}} \right) e^{y\sqrt{\frac{b}{a}}} \operatorname{erfc} \left( \frac{y}{2\sqrt{at}} + \sqrt{bt} \right) \right] \quad (32)$$

$$f_5(y, t) = \operatorname{erfc} \left( \frac{y\sqrt{p_r}}{2\sqrt{t}} \right) \quad (33)$$

$$f_6(y, t) = \frac{e^{a_5 t}}{2} \left[ e^{-y\sqrt{p_r a_5}} \operatorname{erfc} \left( \frac{y\sqrt{p_r}}{2\sqrt{t}} - \sqrt{a_5 t} \right) + e^{y\sqrt{p_r a_5}} \operatorname{erfc} \left( \frac{y\sqrt{p_r}}{2\sqrt{t}} + \sqrt{a_5 t} \right) \right] \quad (34)$$

$$f_7(y, t) = \left( \frac{y^2 p_r}{2} + t \right) \operatorname{erfc} \left( \frac{y\sqrt{p_r}}{2\sqrt{t}} \right) - \frac{y\sqrt{p_r t}}{2\sqrt{\pi}} e^{-\frac{y^2 p_r}{4t}} \quad (35)$$

$$f_8(y, t) = \operatorname{erfc} \left( \frac{y\sqrt{s_c}}{2\sqrt{t}} \right) \quad (36)$$

$$f_9(y, t) = \frac{e^{a_8 t}}{2} \left[ e^{-y\sqrt{s_c a_8}} \operatorname{erfc} \left( \frac{y\sqrt{s_c}}{2\sqrt{t}} - \sqrt{a_8 t} \right) + e^{y\sqrt{s_c a_8}} \operatorname{erfc} \left( \frac{y\sqrt{s_c}}{2\sqrt{t}} + \sqrt{a_8 t} \right) \right] \quad (37)$$

$$f_{10}(y, t) = \left( \frac{y^2 s_c}{2} + t \right) \operatorname{erfc} \left( \frac{y\sqrt{s_c}}{2\sqrt{t}} \right) - \frac{y\sqrt{s_c t}}{2\sqrt{\pi}} e^{-\frac{y^2 s_c}{4t}} \quad (38)$$

Inverse Laplace transform of equations (9) and (10) are

$$\theta(y, t) = f_7(y, t) - f_7(y, t-1)H(t-1) \quad (39)$$

$$C(y, t) = f_{10}(y, t) - f_{10}(y, t-1)H(t-1) \quad (40)$$

And inverse Laplace transform of equation (12) is

$$u(y, t) = g_1(y, t) + h_1(y, t) - h_1(y, t-1)H(t-1) \quad (41)$$

$$\text{Where, } h_1(y, t) = g_2(y, t) + g_3(y, t) + g_4(y, t) \quad (42)$$

$$g_2(y, t) = a_{10}f_1(y, t) + a_{12}f_2(y, t) - a_{14}f_3(y, t) - a_{15}f_4(y, t) \quad (43)$$

$$g_3(y, t) = a_{10}f_5(y, t) - a_{10}f_6(y, t) + a_{11}f_7(y, t) \quad (44)$$

$$g_4(y, t) = a_{12}f_8(y, t) - a_{12}f_9(y, t) + a_{13}f_{10}(y, t) \quad (45)$$

**Solutions for Plate with Constant Temperature:**

In order to understand effects of ramped temperature of the plate on the fluid flow, we must compare our results with constant temperature. In this case, the initial and boundary conditions are the same excluding Eq. (8) that becomes  $\theta = 1$  at  $y = 0, t \geq 0$ . We find the isothermal temperature  $\theta(y, t)$  using Laplace transform.

$$\theta(y, t) = f_5(y, t) \quad (46)$$

Similarly, Velocity  $u(y, t)$  for plate with constant temperature using the Laplace transforms technique

$$u(y, t) = g_1(y, t) + h_2(y, t) + h_3(y, t) - h_3(y, t - 1)H(t - 1) \quad (47)$$

$$\text{Where, } h_2(y, t) = g_5(y, t) + g_7(y, t) \quad (48)$$

$$h_3(y, t) = g_6(y, t) + g_4(y, t) \quad (49)$$

$$g_5(y, t) = a_{11}f_1(y, t) - a_{11}f_3(y, t) \quad (50)$$

$$g_6(y, t) = a_{12}f_2(y, t) - a_{12}f_3(y, t) - a_{13}f_4(y, t) \quad (51)$$

$$g_7(y, t) = a_{11}f_5(y, t) - a_{11}f_6(y, t) \quad (52)$$

**Solutions for Plate with Constant Surface Concentration:**

$$C(y, t) = f_8(y, t) \quad (53)$$

$$u(y, t) = g_1(y, t) + h_4(y, t) + h_5(y, t) - h_5(y, t - 1)H(t - 1) \quad (54)$$

$$\text{Where, } h_4(y, t) = g_8(y, t) + g_{10}(y, t) \quad (55)$$

$$h_5(y, t) = g_9(y, t) + g_3(y, t) \quad (56)$$

$$g_8(y, t) = a_{13}f_2(y, t) - a_{13}f_3(y, t) \quad (57)$$

$$g_9(y, t) = a_{10}f_1(y, t) - a_{10}f_3(y, t) - a_{11}f_4(y, t) \quad (58)$$

$$g_{10}(y, t) = a_{13}f_8(y, t) - a_{13}f_9(y, t) \quad (59)$$

**Solutions for Plate with Constant Temperature and Constant Surface Concentration:**

$$\theta(y, t) = f_5(y, t) \quad (60)$$

$$C(y, t) = f_8(y, t) \quad (61)$$

$$u(y, t) = g_1(y, t) + h_6(y, t) \quad (62)$$

$$\text{Where, } h_6(y, t) = g_{11}(y, t) + g_7(y, t) + g_{10}(y, t) \quad (63)$$

$$g_{11}(y, t) = a_{11}f_1(y, t) + a_{13}f_2(y, t) - a_{15}f_3(y, t) \quad (64)$$

**Results and discussion:**

In order to understand the physical aspects of the problem, a parametric study is performed and the numerical results are elucidated with the help of graphical illustrations. We have presented the non-

dimensional fluid velocity, fluid temperature and concentration for several values of Prandtl number  $Pr$ , Grashof number  $Gr$ ,  $Gm$ , Casson parameter  $\gamma$ , magnetic parameter  $M$ , permeability of porous medium  $K$  and time  $t$  in Figs. 1-12. Fig. 1 shows the effect on velocity profiles for different values of Casson parameter  $\gamma$ , when the other parameters are fixed. It is observed that velocity of the fluid decreases with increasing values Casson parameter  $\gamma$ . An increase in Casson parameter makes the velocity boundary layer thickness shorter. Thus, the velocity boundary layer thickness for Casson fluid is larger than the Newtonian fluid. It occurs because of plasticity of Casson fluid. When Casson parameter decreases the plasticity of the fluid increases, which causes the increment in velocity boundary layer thickness. It is also observed that velocity profile is lower in case of ramped wall temperature as compare to isothermal temperature. The influence of magnetic parameter  $M$  on velocity profiles is shown in Fig. 2. It is observed that velocity decreases with increasing values of  $M$ . It is observed that the amplitude of the velocity as well as the boundary layer thickness decreases when  $M$  is increased. Physically, it may also be expected due to the fact that the application of a transverse magnetic field results in a resistive type force (called Lorentz force) similar to the drag force, and upon increasing the values of  $M$ , the drag force increases which leads to the deceleration of the flow.

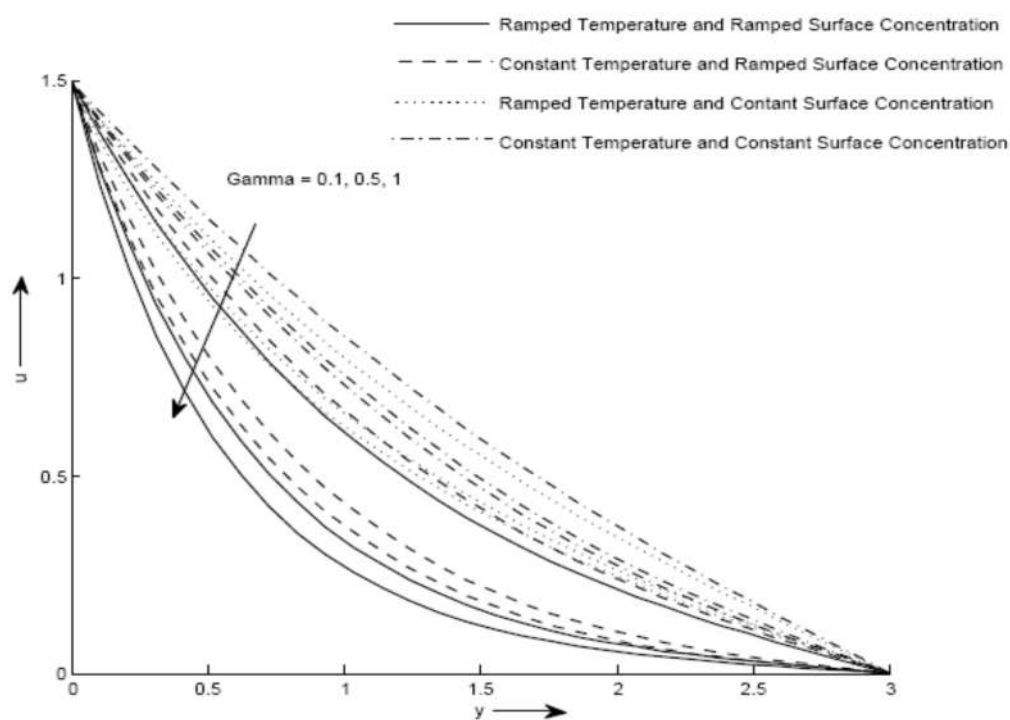


**Fig 1 : Velocity profile  $u$  for different values of  $y$  and  $\gamma$  at  $M = 0.5$ ,  $Sc = 0.2$ ,  $Gm = 10$ ,  $Gr = 5$ ,  $Pr = 0.71$ ,  $k = 0.1$  and  $t = 0.4$**



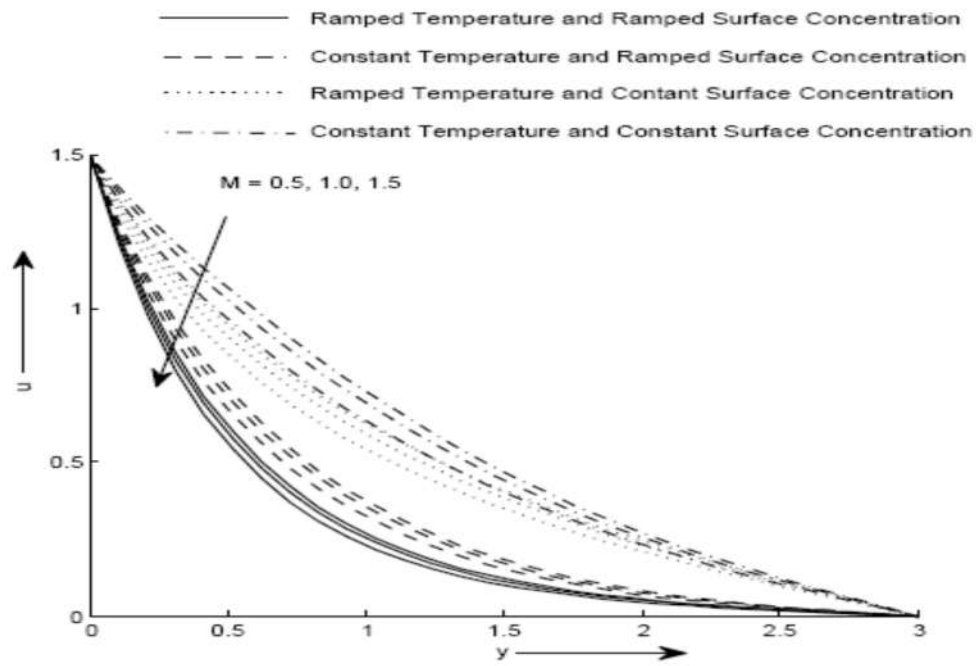


**Fig 2: Velocity profile  $u$  for different values of  $y$  and  $M$  at  $Pr = 0.71, Sc = 0.2, k = 0.1$   
 $Gr = 5, Gm = 10, \gamma = 1$  and  $t = 0.4$**

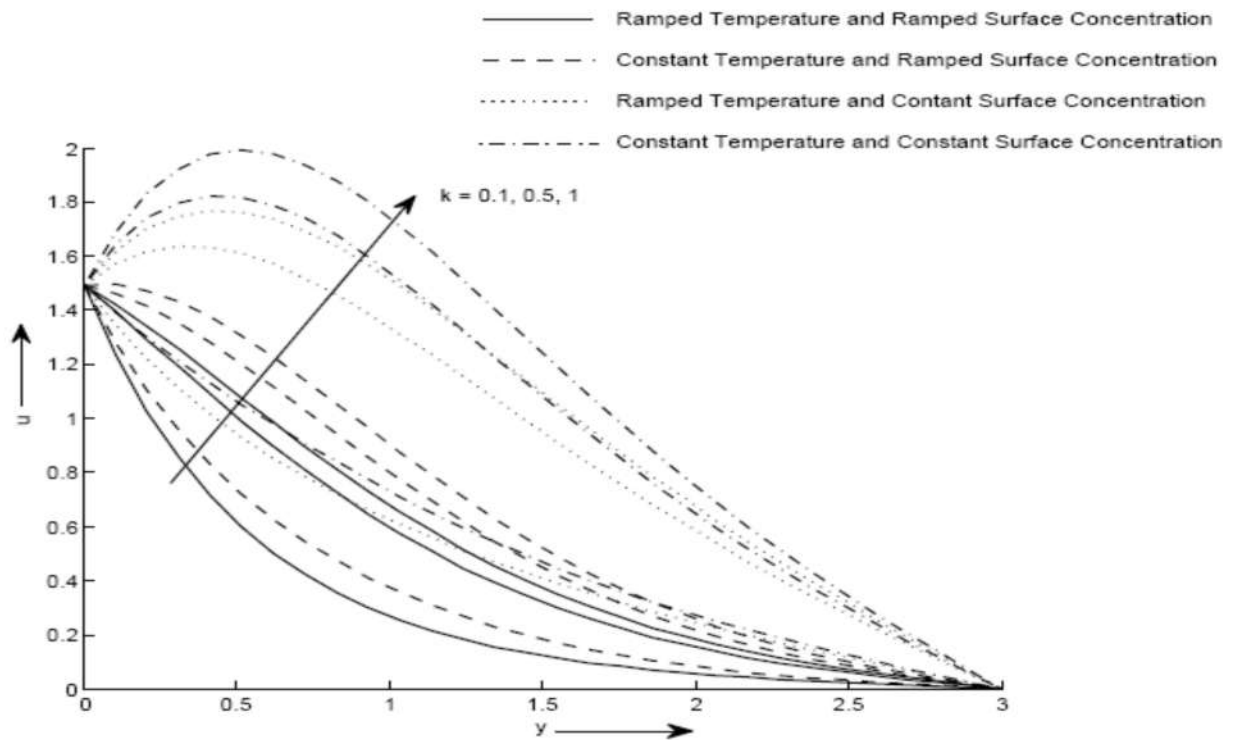


**Fig 3: Velocity profile  $u$  for different values of  $y$  and  $K$  at  $M = 0.5, \gamma = 1, Pr = 0.71, Sc = 0.2, Gr = 5, Gm = 10$  and  $t = 0.4$**

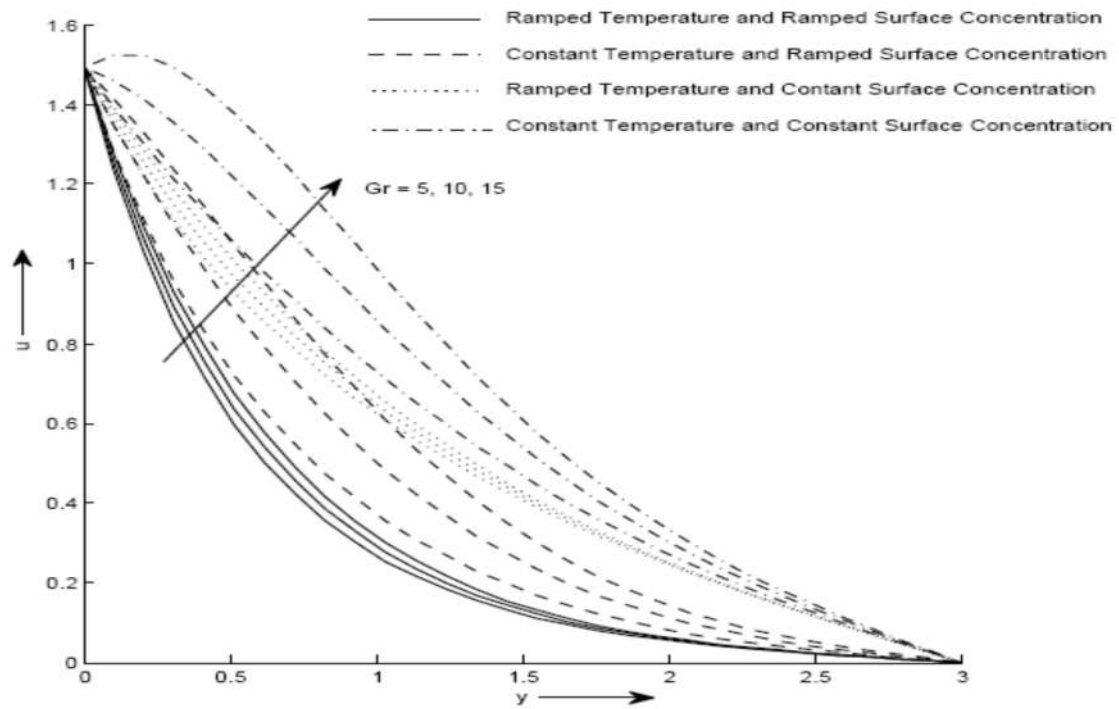


**Fig 4: Velocity profile  $u$  for different values of  $y$  and  $Gr$  at  $M = 0.5$ ,  $Sc = 0.2$ ,  $Gm = 10$ ,  $Pr = 0.71$ ,  $\gamma = 1$ ,  $k = 0.1$  and  $t = 0.4$**

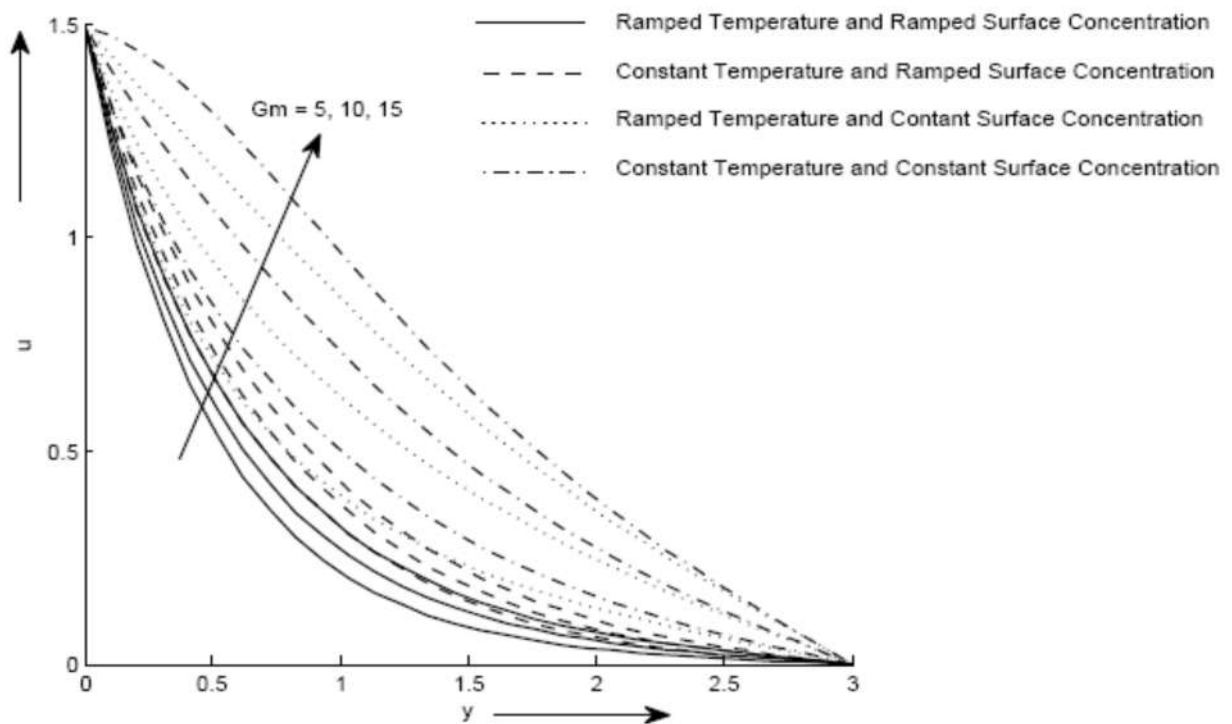


**Fig 5: Velocity profile  $u$  for different values of  $y$  and  $Gm$  at  $M = 0.5$ ,  $Gr = 5$ ,  $k = 0.1$ ,  $Pr = 0.7$ ,  $\gamma = 1$ ,  $Sc = 0.2$  and  $t = 0.4$**

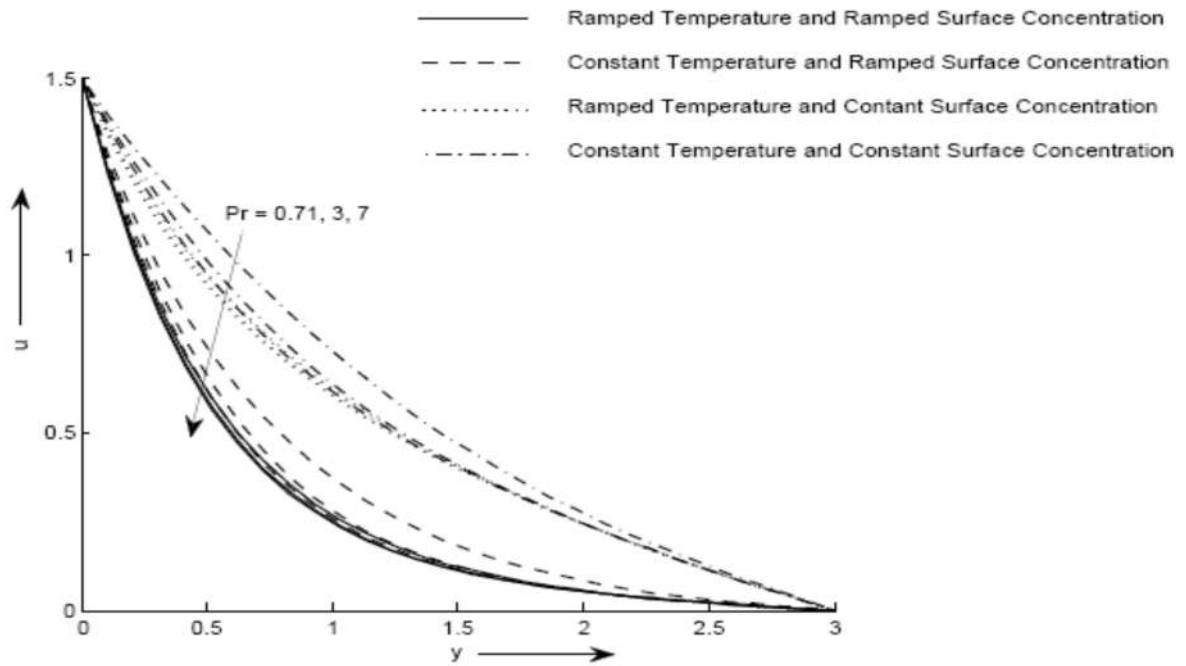


Fig 6: Velocity profile  $u$  for different values of  $y$  and  $Pr$  at  $M = 0.5, k = 0.1, Gr = 5, Gm = 10, Sc = 0.2, \gamma = 1$  and  $t = 0.4$

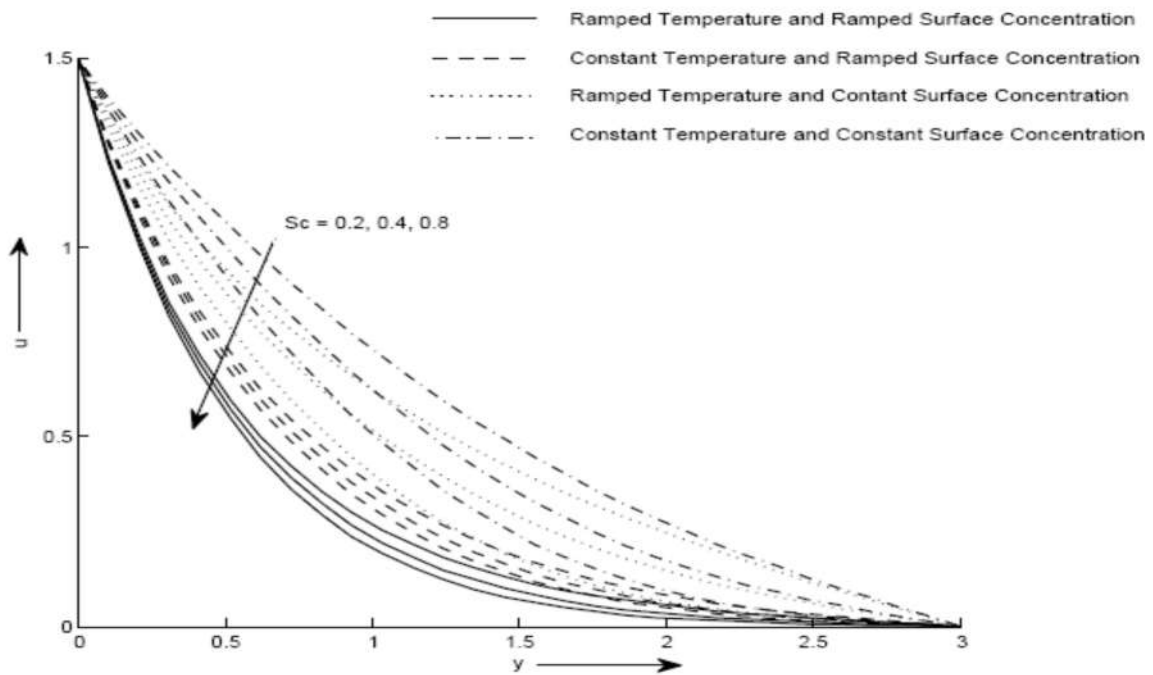
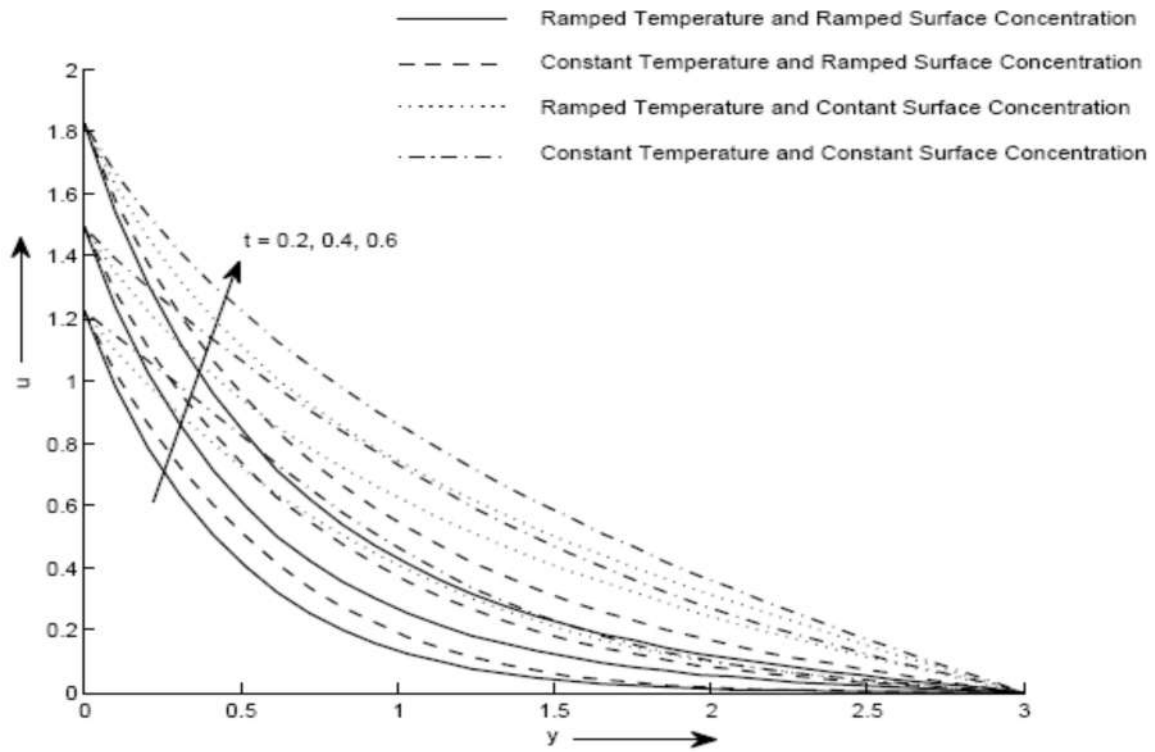
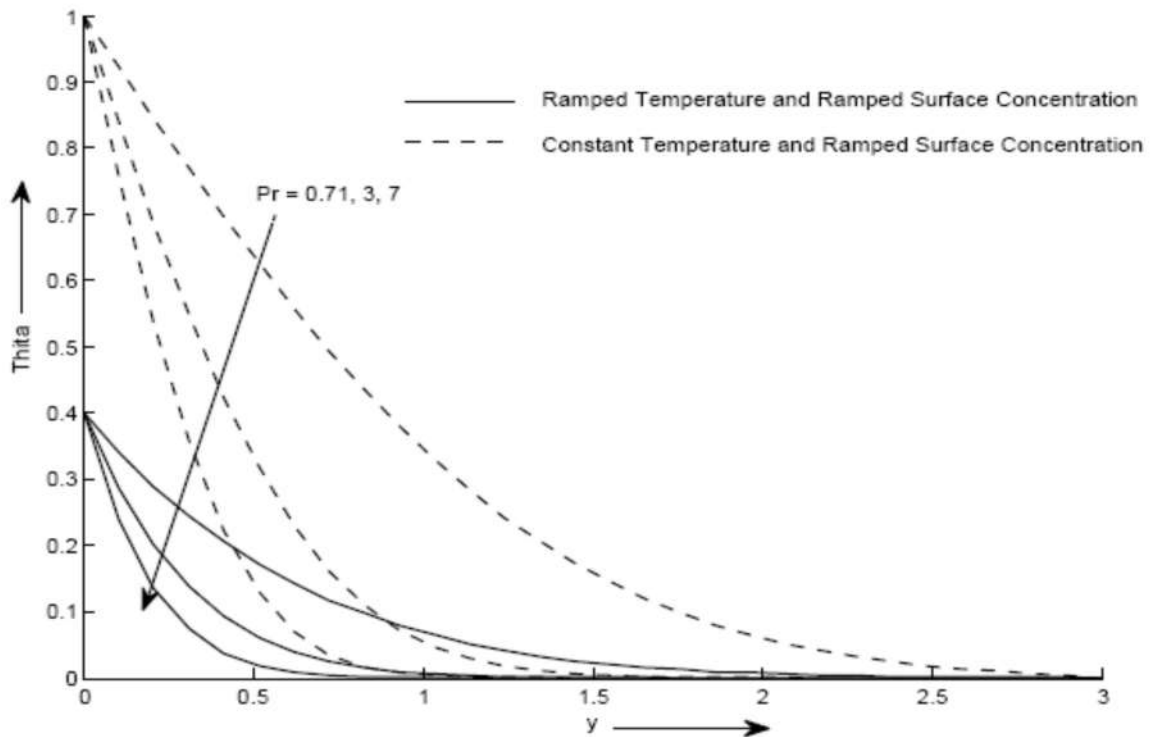


Fig 7: Velocity profile  $u$  for different values of  $y$  and  $Sc$  at  $M = 0.5, k = 0.1, Gr = 5, Gm = 10, Pr = 0.71, \gamma = 1$  and  $t = 0.4$



**Fig 8: velocity profile  $u$  for different values of  $y$  and  $t$  at  $M = 0.5, Sc = 0.2, Gm = 10, k = 0.1$   
 $Gr = 5, Pr = 0.71$  and  $\gamma = 1$**



**Fig 9: Temperature profile  $\theta$  for different values of  $y$  and  $Pr$  at  $M = 0.5, Sc = 0.2, Gm = 10,$   
 $k = 0.1, t = 0.4, Gr = 5$  and  $\gamma = 1$**

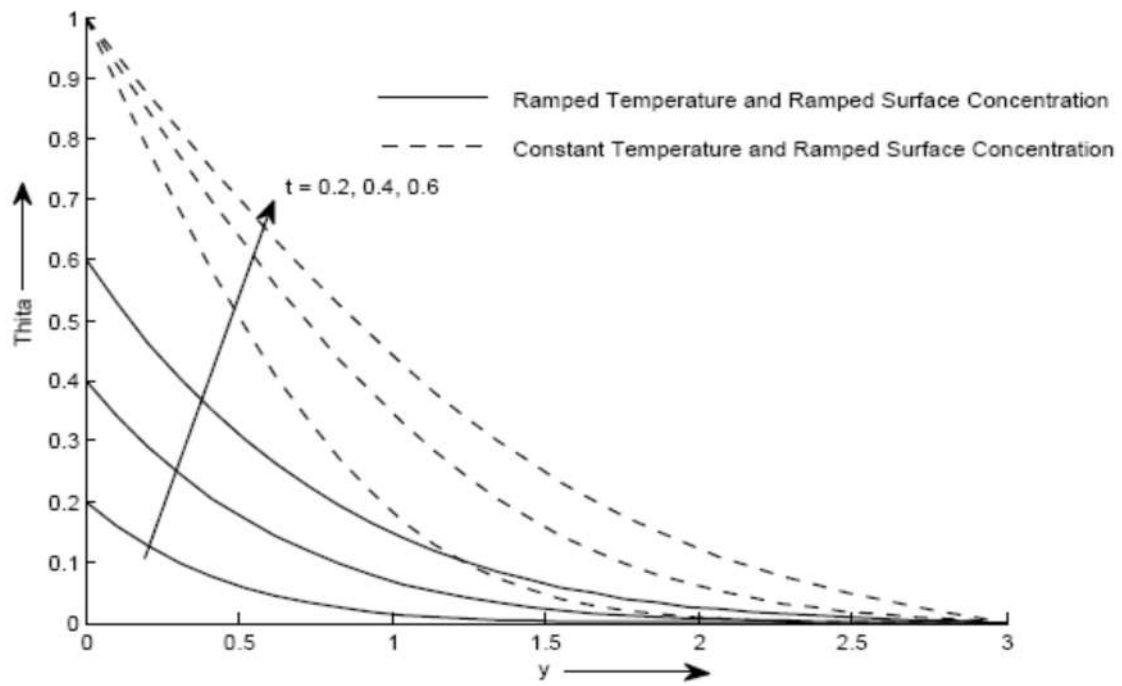


**Fig 10: Temperature profile  $\theta$  for different values of  $y$  and  $t$  at  $M = 0.5, Sc = 0.2, Gm = 10, k = 0.1, Gr = 5, Pr = 0.71$  and  $\gamma = 1$**

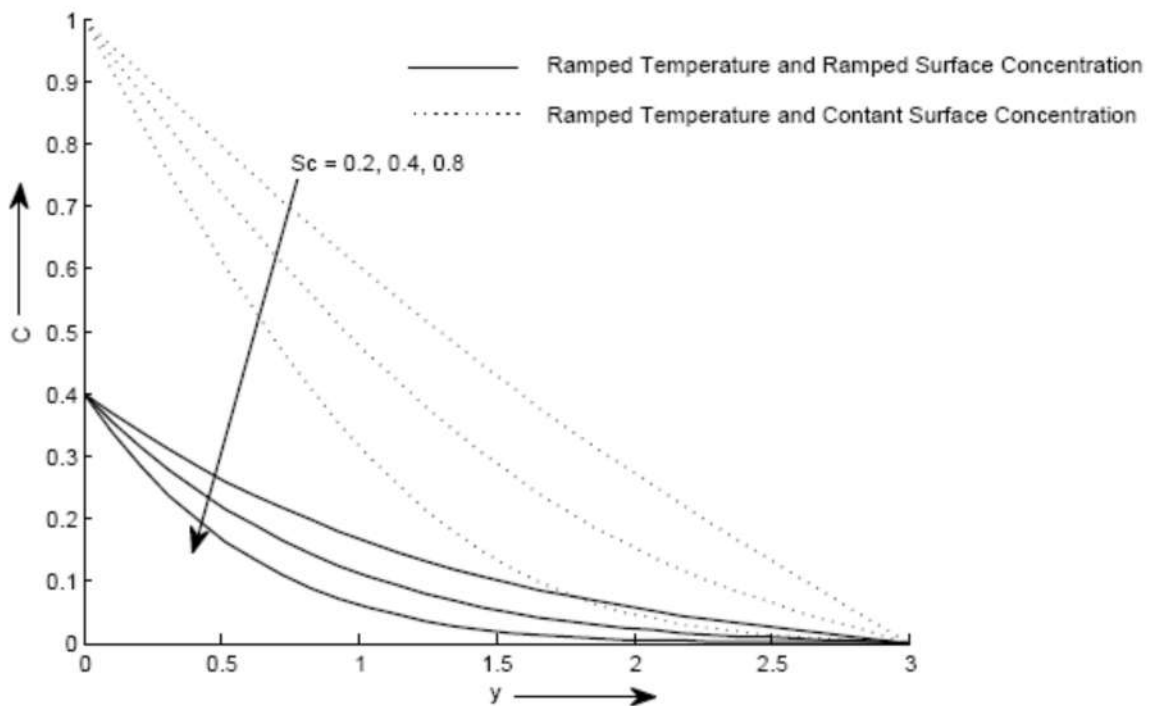


**Fig 11: Concentration profile  $C$  for different values of  $y$  and  $Sc$  at  $Pr = 0.71, k = 0.1, t = 0.4, Gm = 10, Gr = 5, M = 0.5$  and  $\gamma = 1$**

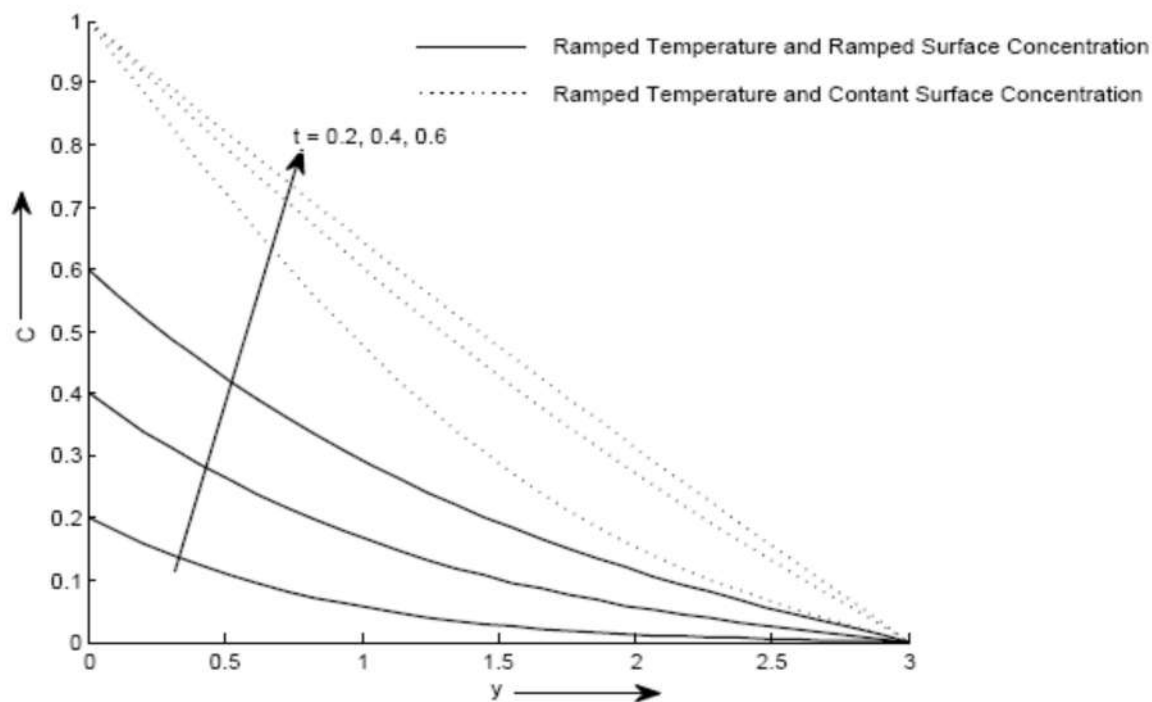


**Fig 12: Concentration profile  $C$  for different values of  $y$  and  $t$  at  $Pr = 0.71, Sc = 0.2, k = 0.1$   
 $Gm = 10, Gr = 5, \gamma = 1$  and  $M = 0.5$**

Fig. 3 shows the effect of permeability of porous medium  $K$  on the velocity of the fluid. It shows that velocity increase with increase in the value of  $K$ . It obvious that velocity of the fluid increase with increasing porosity of the medium. In Fig. 4, velocity has been plotted for various values of Grashof number  $Gr$ . It is observed that velocity increases with increasing values of  $Gr$ . The flow is accelerated due to the enhancement in the buoyancy forces corresponding to the increasing values of Grashof number. In Fig. 5, the velocity profile has been plotted for various values of Mass Grashof number  $Gm$ . It observed that the velocity increase with the increase in the value of  $Gm$ . From Fig. 6, it can be observed that velocity profile decreases as increasing the value of Prandtl number  $Pr$ . The graphical results for  $Sc$  are shown in Fig. 7. It is observed that the fluid velocity decreases with increase in  $Sc$ . In Fig. 8, velocity profile shows for different values for time  $t$ . It is observed that the velocity is an increasing function of time  $t$ . It is obvious from Fig. 9, the temperature decreases as the Prandtl number  $Pr$  increases. It is justified due to the fact that thermal conductivity of the fluid decreases with increasing Prandtl number  $Pr$ . Fig. 10 illustrate the effects of the dimensionless time  $t$  on the temperature profiles. Obviously the temperature increases with increasing time  $t$ . by keeping other parameters fixed. Fig. 11 indicates that, concentration decreases with increasing values of  $Sc$ . Fig. 12 shows the effect on concentration profile for different value of time, it has been seen that concentration increase with increase in  $t$ .

### Conclusion:

The purpose of this study is to obtain exact solutions for the unsteady natural convective casson fluid flow past over an exponentially accelerated vertical plate in the presence of a transverse uniform magnetic field. The expressions for the velocity, temperature and concentration have been obtained in closed form with the help of the Laplace transform technique. The effects of the different parameters on velocity, temperature and concentration profiles are presented graphically. The most important concluding remarks can be summarized as follows:

- Velocity of the fluid decreases with increasing in casson parameter  $\gamma$ .
- Velocity decreases with increasing values of magnetic parameter  $M$ .
- For large values of permeability parameter  $K$ , velocity increase
- Velocity increases with increasing values of Grashof number  $G_m$  and  $G_r$ .
- The fluid velocity decreases with increase in Prandtl number  $Pr$ .
- Velocity decrease with increase in Schmidt number  $Sc$ .
- Velocity is an increasing function of time  $t$ .
- Temperature decreases as the Prandtl number  $Pr$  increases.
- Temperature increases with increasing time  $t$ .
- Concentration decreases with increase in Schmidt number  $Sc$ .
- Concentration increases with increase in  $t$ .

### References:

- [1] Hartmann, J., (1937): Hg-dynamics I theory of the laminar flow of an electrically conductive liquid in a homogenous magnetic field, *DetKal. Danske Videnskabernes Selskab, Matematisk-fysiske Meddeleser*, XV, 1-27.
- [2] Alfven, H., (1942): Existence of electromagnetic-hydrodynamic waves, *Nature*, 150, 405-406.
- [3] H. R. Kataria, A. Mittal, (2015): Mathematical model for velocity and temperature of gravity-driven convective optically thick nanofluid flow past an oscillating vertical plate in presence of magnetic field and radiation. *Journal of Nigerian Mathematical Society*, 34, 303– 317.
- [4] H. R. Kataria, A. S. Mittal, (2017): Velocity, mass and temperature analysis of gravity driven convection nanofluid flow past an oscillating vertical plate in presence of magnetic field in a porous medium, *Applied Thermal Engineering*, 110, 864-874.
- [5] M. Sheikholeslami, T. Hayat, A. Alsaedi, (2017): Numerical simulation of nanofluid forced convection heat transfer improvement in existence of magnetic field using Lattice Boltzmann Method, *International Journal of Heat and Mass Transfer*, 108, 1870-1883.
- [6] H. R. Kataria, H. R. Patel, (2015): Effect of magnetic field on unsteady natural convective flow of a micropolar fluid between two vertical walls. *Ain Shams Engineering Journal*, doi. 10.1016/j.asej.2015.08.013.

- [7] H. R. Kataria, H. R. Patel, (2016): Effect of thermo-diffusion and parabolic motion on MHD Second grade fluid flow with ramped wall temperature and ramped surface concentration, *Alexandria Engineering Journal*, 10.1016/j.aej.2016.1
- [8] H. R. Kataria, H. R. Patel, (2016): Heat and Mass Transfer in MHD Second Grade Fluid Flow with Ramped Wall Temperature through Porous Medium, *Mathematics Today Vol.32* 67-83.
- [9] T. Hayat, I. Naeem, M. Ayub, A.M. Siddiqui, S. Asghar, C.M. Khaliq, (2009): Exact solutions of second grade aligned MHD fluid with prescribed vorticity, *Nonlinear Analysis: Real World Applications*, 10, 2117–2126
- [10] T. Hayat, I. Ullah, T. Muhammad, A. Alsaedi, (2016): Magnetohydrodynamic (MHD) three-dimensional flow of second grade nanofluid by a convectively heated exponentially stretching surface, *Journal of Molecular Liquids*, 220, 1004–1012
- [11] A. S. Bataineh, O.R. Isik, I. Hashim, (2016): Bernstein method for the MHD flow and heat transfer of a second grade fluid in a channel with porous wall, *Alexandria Engineering Journal*, <http://dx.doi.org/10.1016/j.aej.2016.06.022> 1110-0168
- [12] H. R. Kataria, H. R. Patel, (2016): Radiation and chemical reaction effects on MHD Casson fluid flow past an oscillating vertical plate embedded in porous medium, *Alexandria Engineering Journal* , 55, 583-595
- [13] H. R. Kataria, H. R. Patel, (2016): Soret and heat generation effects on MHD Casson fluid flow past an oscillating vertical plate embedded through porous medium, *Alexandria Engineering Journal*, 55, 2125–2137
- [14] M. Y. Malik, Mair Khan, T. Salahuddin, Imad Khan, (2016): Variable viscosity and MHD flow in Casson fluid with Cattaneo–Christov heat flux model: Using Keller box method, *Engineering Science and Technology*, 1985-1992.
- [15] S. Nadeem, R.U. Haq, C. Lee, (2012): MHD flow of a Casson fluid over an exponentially shrinking sheet, *Sci. Iran.*, 19, 1550–1553
- [16] S. Nadeem, R.U. Haq, N.S. Akbar, Z.H. Khan, (2013): MHD three-dimensional Casson fluid flow past a porous linearly stretching sheet, *Alexandria Eng. J.*, 52, 577–582.
- [17] S. Mukhopadhyaya, I.C. Moindala, T. Hayat, (2014): MHD boundary layer flow of Casson fluid passing through an exponentially stretching permeable surface with thermal radiation, *Chin. Phys.*, 23, 104701
- [18] S. Mukhopadhyay, P.R. De, K. Bhattacharyya, G.C. Layek, (2013): Casson fluid flow over an unsteady stretching surface, *Ain Shams Eng. J.*, 4, pp. 933–938
- [19] Asma Khalid, Ilyas Khan, Arshad Khan, Sharidan Shafie, (2015): Unsteady MHD free convection flow of Casson fluid past over an oscillating vertical plate embedded in a porous medium, *Engineering Science and Technology*, 309-317.
- [20] Rosseland S. (1931): *Astrophysik und atom-theoretische Grundlagen*. Berlin: Springer-Verlag.